Crystal Structure and Magnetic Properties of the Quasi-One-Dimensional Compound $(Ca_{1-x}Y_x)_{0.82}CuO_2$ Prepared at Room Pressure

Yuzuru Miyazaki,[a] Neil C. Hyatt,[a] Marcin Slaski,[b] Ian Gameson,[a] and Peter P. Edwards*[a]

Abstract: A solid solution of the quasi-one-dimensional cuprate, $(Ca_{1-x}Y_x)_{0.82}CuO_2$ with $0 \le x \le 0.435$, has been successfully synthesized at room pressure. Upon yttrium doping (decreasing hole concentration), the formal Cu valence of the solid solution changes from $+2.36$ to $+2.00$ without any significant change in the crystal structure. The solid solution shows an evolution in magnetic behavior, from a dimerlike spin state to a long-range, magnetically ordered state. The former state can be treated as a dilute one-dimensional spin system consisting of both spin dimers ($S = 0$) and paramagnetic spin segments ($S = 1/2$).

Keywords: crystal engineering · cuprates · low-dimensional compounds · magnetic properties · solid solution

Introduction

Since the discovery of superconductivity at $T = 12$ K in the spin-ladder compound $(Sr,Ca)_{14}Cu_{24}O_{41}$,[1] cuprates that exhibit a so-called spin-gap state with low-dimensional Cu–O networks have been extensively studied.[2] The crystal structure of $(Sr,Ca)_{14}Cu_{24}O_{41}$ consists of two distinct Cu–O networks as shown in Figure 1.[3] One is a Cu_2O_3 ladder composed of two edge-shared zig-zag chains; the other is an edge-shared CuO_2 square-planar chain, as seen in the $NaCuO_2$-type structure.[4] These ladders and chains stack alternatively along the *b* axis to form a low-dimensional structure. Although the formal valence state of Cu is $+2.25$ in $Sr_{14}Cu_{24}O_{41}$, the compound shows semiconducting behavior due to the complete localization of hole carriers within the CuO_2 chains. When Sr sites are partially substituted by Ca ions, electronic charge transfer from the CuO_2 chains to the Cu_2O_3 ladders occurs and subsequently the compound becomes conductive. Kato and co-workers[5, 6] examined the magnetic susceptibility of the solid solution $(Sr,Ca)_{14}Cu_{24}O_{41}$ and found a broad peak at a temperature around 80 K. They attributed this to spin-gap behavior within the CuO_2 chains, since it is generally assumed that the vast majority of spins on the Cu^{2+} sites in the Cu_2O_3 ladders have already formed spin-singlet pairs ($S = 0$) at room temperature. It is now believed that there are two distinct spin gaps with associated gap energies of ~ 100 K (CuO_2 chains) and ~ 500 K (Cu_2O_3 ladders), respectively, in this compound.[7] Thus, the existence of both ladders and chains in $(Sr,Ca)_{14}Cu_{24}O_{41}$ makes for a complicated electronic structure. Actually there exist compounds in the Sr–Cu–O system that have either Cu_2O_3 ladders or CuO_2 chains, namely $SrCu_2O_3$[8] and $Sr_{0.73}CuO_2$,[9] respectively. Unfortunately, to date, both compounds have only been synthesized under high applied pressures. The compound $Ca_{1-y}CuO_2$ ($y \sim 0.15$),[10, 11] on the other hand, which has the one-dimensional edge-shared CuO_2 chains, can be synthesized at room pressure. In Figure 2 we show the crystal structure of $Ca_{1-y}CuO_2$; this structure is essentially identical to those of $Sr_{0.73}CuO_2$ and $Ba_{0.67}CuO_2$.[12] Since these alkaline-earth cuprates appear to have an in-built cation deficiency,[9–12] an incommensurate superstructure

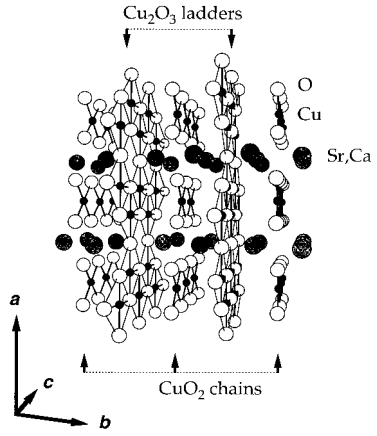

Figure 1. The crystal structure of $(Sr,Ca)_{14}Cu_{24}O_{41}$ viewed in perspective along the *c* axis.

[a] Prof. P. P. Edwards, Dr. I. Gameson, Dr. Y. Miyazaki, N. C. Hyatt
School of Chemistry, University of Birmingham
Birmingham B15 2TT (UK)
Fax: (+44) 121-414-4442
E-mail: p.p.edwards@bham.ac.uk

[b] Dr. M. Slaski
School of Physics and Astronomy, University of Birmingham
Birmingham B15 2TT (UK)

  0947-6539/99/0508-2265 $ 17.50+.50/0

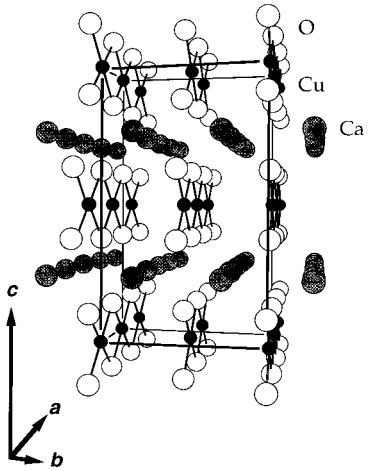

Figure 2. The orthorhombic basic structure of $Ca_{1-y}CuO_2$ viewed in perspective along the *a* axis. In the actual structure, the CuO_2 chains are slightly twisted.

arises due to the periodic differences in arrangements of the alkaline-earth cations and the CuO_2 chains. As a result of this cation deficiency, the oxidation state of Cu always appears above +2.0, even without substantial changes in the oxygen stoichiometry. For example, the formal Cu valence of $Ca_{0.85}CuO_2$ is found to be +2.3, which implies that excess holes must be introduced into the electronically active CuO_2 chains. However, the mixed-valent compound is an insulator, owing to localization of the introduced holes. Davies and colleagues[13, 14] have reported that a certain amount of Y ions (also Nd and Gd ions) can substitute for the Ca site to form a solid solution; this is generally represented as $Ca_{2+x}Y_{2-x}Cu_5O_{10}$ ($0 \le x \le 0.8$), rather than $(Ca_{1-x}Y_x)_{1-y}CuO_2$. The formal valence of Cu in the solid solution varies from 2.00 to 2.16.

It is interesting to see how the magnetic structure evolves in such a solid solution with a one-dimensional CuO_2 network, in which the formal Cu valence changes without any significant change in the crystal structure. We have succeeded in preparing, at room pressure, the solid solution of formula $(Ca_{1-x}Y_x)_{1-y}CuO_2$ over a large substitutional range and we have measured the temperature dependence of the magnetic susceptibility. During the course of our experiments, Dolinsek and co-workers[15] reported the magnetic susceptibility of $Ca_{0.85}CuO_2$, which showed a broad maximum at around 50 K. These authors have proposed that the broad peak is attributed not to the spin dimer but to even-number spin fragments. We are also aware of the recent work of Hayashi and co-workers,[16] using high-pressure synthesis (at 215 bar of oxygen), who present complementary results to our own. Interestingly, our room-pressure synthesis appears to be highly successful in producing high phase purity over a relatively wide solid-solution range. In the present paper, we report the synthesis of the solid solution $(Ca_{1-x}Y_x)_{0.82}CuO_2$, with $0 \le x \le 0.435$, prepared at room pressure. We also report an accompanying structural analysis and magnetic properties across the solid-solution range, and compare our results with those for materials synthesized under high oxygen pressure by Hayashi and co-workers.[16]

Results and Discussion

In Figure 3 we show the composition diagram for $(Ca_{1-x}Y_x)_{1-y}CuO_2$ in terms of the compositional parameters $(1-y)$ and x. Oblique lines in the figure indicate the formal Cu valences calculated from the nominal compositions. We

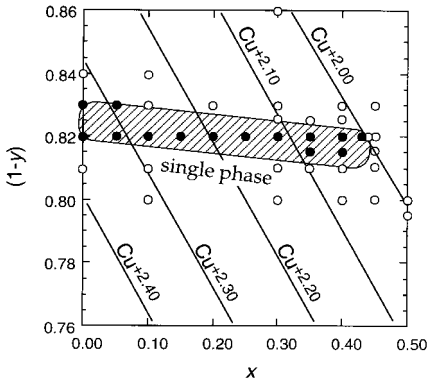

Figure 3. The $(1-y)$ vs. x compositional diagram for the $(Ca_{1-x}Y_x)_{1-y}CuO_2$ solid solution. Shaded area represents the region where the single-phase samples are prepared. Open circles indicate that the samples contain an impurity phase(s).

have succeeded in preparing single-phase samples over a wide range of yttrium composition x, as shown by the filled circles in Figure 3. Although single-phase samples could be prepared at $(1-y) \sim 0.80$, the widest single-phase region (shaded area) was obtained at $(1-y) = 0.82$. Thus, detailed results are presented here for the formula $(Ca_{1-x}Y_x)_{0.82}CuO_2$, with $0 \le x \le 0.435$. Thermogravimetric measurements confirmed that the oxygen content of all the single-phase samples remained at 2.00, within experimental error. Hence, we treat the solid solution with no oxygen deficiency and the nominal Cu valence ranges from +2.36 ($x = 0$) to +2.00 ($x = 0.435$). Whenever we attempted to synthesize the samples at $(1-y) = 0.80$, which corresponds to the formula of $Ca_{2+x}Y_{2-x}Cu_5O_{10}$ reported previously by Davies,[14] we invariably found, from powder X-ray diffraction, small but clearly discernable amounts of impurities (e.g., CuO and $Cu_2Y_2O_5$). This discrepancy in the single-phase composition might be attributed to the preparation conditions, in particular oxygen partial pressures. We also found impurities in the whole electron-doped region of $Cu^{n+} < +2.00$.

In Figure 4 we show the effect of yttrium substitution on the lattice parameters of the basic cell of the samples, as refined by the X-ray Rietveld method.[17] The magnitude of estimated standard deviations (esd's) of all the values are within the data points shown. For comparison, the results reported under 215 bar of oxygen by Hayashi and co-workers,[16] are also shown. Although the nominal stoichiometry reported by those authors is different from our own, we recalculated their data so as to represent the relative Y content (x). The crystal *a*-axis length, which relates to the nearest Cu–Cu distance along the chain direction (see Figure 2), gradually increases with increasing x and appears to saturate at higher x values. The substitution of smaller trivalent Y ions for divalent Ca has a marked effect on the length of the *b*-axis, while the length of the *c* axis remains almost constant. Similar size effects have been also observed for the samples prepared under high

0947-6539/99/0508-2266 $ 17.50+.50/0 *Chem. Eur. J.* **1999**, *5*, No. 8

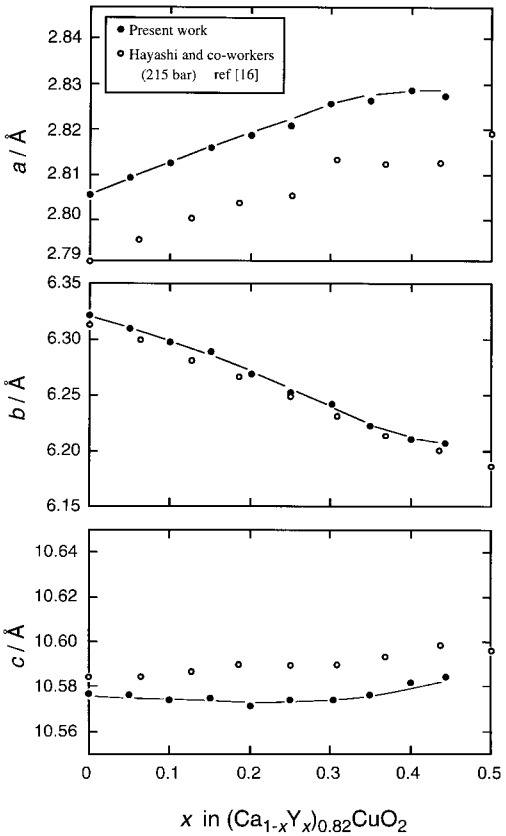

Figure 4. Effect of the yttrium substitution on the lattice parameters of $(Ca_{1-x}Y_x)_{0.82}CuO_2$.

oxygen pressure.[16] The differences in the absolute values of those lattice parameters can be rationalized in terms of the differences in both pressure and composition. The cell volume calculated from these lattice parameters monotonically decreased from a value of 187.6(1) Å^3 ($x = 0$) to 185.8(1) Å^3 ($x = 0.435$); these values were consistently about 0.5% larger than those reported by Hayashi and co-workers.[16] Our detailed structural work including the incommensurate superstructure will be presented elsewhere. Briefly, upon Y doping, the Cu–O distance in the CuO_2 chain gradually increases from a value of 1.932(2) Å to 1.976(4) Å, while the next-nearest Cu–Cu distance (interchain) decreases continuously from 3.458(1) Å to 3.410(1) Å. The modulation periods along the a axis changes from 6.02(5)a to 5.16(5)a; this approximately represents the stoichiometry of the samples, varying from $Ca_{0.834}CuO_2$ [$Ca_{1-1/6.02}CuO_2$] to $(Ca,Y)_{0.806}CuO_2$ [$Ca_{1-1/5.16}CuO_2$] even when we prepared all the samples with the $(Ca,Y)_{0.82}CuO_2$ composition. Large changes in the incommensurate periods along the c axis [from 6.29(1)c to 3.97(1)c] could compensate for this compositional and periodic discrepancy. Interestingly, although the crystal structural change is small and continuous, the solid solution shows a distinct transition in magnetic behavior upon Y doping, from a dimerlike state to a long-range magnetically ordered state. As has just recently been reported by Hayashi and co-workers,[16] the samples with $x \leq 0.15$ show a broad peak in the $\chi - T$ curves (T_{peak}) below 40 K, while the samples with $0.20 \leq x \leq 0.435$ show a clear antiferromagnetic transition (T_N) below 30 K. In Figure 5 we show the variation of T_N and T_{peak} against

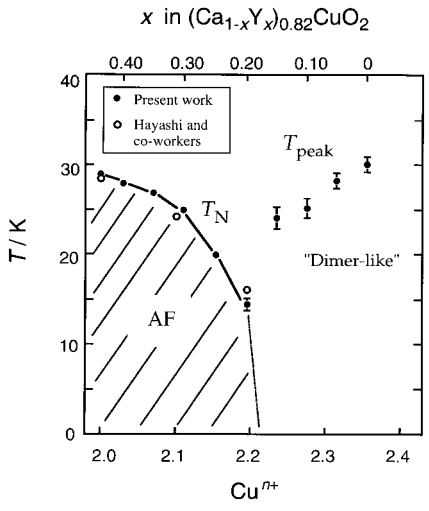

Figure 5. Magnetic phase diagram of $(Ca_{1-x}Y_x)_{0.82}CuO_2$.

the formal Cu valences of the samples (Cu^{n+}) together with the recently reported results from other groups. The sample with $x = 0.435$ has no excess charge (namely, $Cu^{n+} = 2.00$) and has a T_N of 29 K, and can be regarded as a parent compound of the system. As the carrier doping increases (decreasing x), T_N gradually decreases and vanishes at around $Cu^{n+} = 2.20$. Then, a dimerlike state emerges with a further decrease in the compositional parameter x. Despite the vastly different preparation conditions between our own studies and Hayashi and co-workers,[16] the similar behavior of the samples implies that the carrier concentration is the key factor in dictating the magnetic behavior. To fully interrogate the cross-over region of the magnetic behavior, ESR and neutron scattering experiments for the samples of $x \sim 0.15$ are currently underway.

In Figure 6 we show schematically probable spin configurations on 2×10 Cu sites along the CuO_2 chains for each carrier doping state (spin directions are not taken into

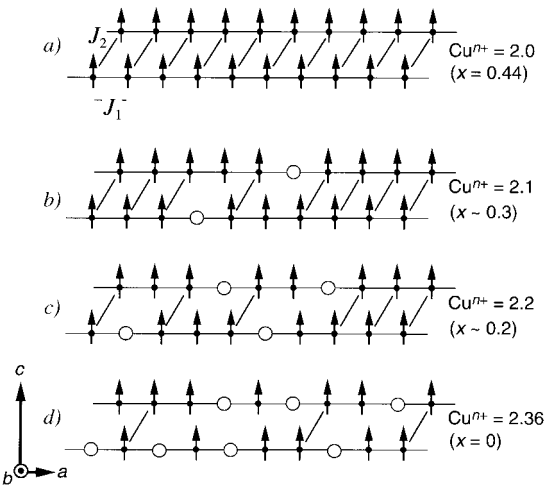

Figure 6. Schematic representations of possible spin configurations upon carrier doping. Open circles represent so-called Zhang–Rice singlets. Spin directions are not taken into account.

account). For clarity the oxygen atoms have been omitted. The O–Cu–O angles are almost 90° in the solid solution, and hence the superexchange coupling between the nearest

neighbor Cu atoms, here taken as J_1, can be substantially weaker than that of Sr_2CuO_3 with $J_1 \sim 2200$ K,[18] in which the O–Cu–O angles are 180°. Then, the direct coupling between the CuO_2 chains (interchain), J_2, must be significant, since the interchain Cu–Cu distance is only about 3.41 Å. This length is apparently longer than the nearest Cu–Cu distance along the chain of 2.81 Å (= a), but much shorter than that of the next-nearest one of 5.62 Å (= $2a$). Two other Cu–Cu distances are around 5.3 Å and are neglected in this report for simplicity. Through carrier doping, the spin configurations might vary from states (a) to (d) as shown in Figure 6. The doped hole carriers might mainly form magnetically inactive Zhang–Rice[19] spin singlets, shown by open circles. As the number of these singlets increases, the long-range-ordered state collapses gradually and causes a decrease of T_N. Between the states (c) and (d), the interchain coupling, J_2, might become significantly small relative to that of the state (a), and thus each CuO_2 chain can be treated as an isolated entity. Actually, T_N vanishes at around this composition and another state, a dimerlike state, appears. In the vicinity of the magnetic state (d), Zhang–Rice singlets are located at almost every third site. We performed curve-fittings on the susceptibility data for the sample with $x = 0$, using both a noninteracting dimer model[20] and an alternating chain model.[21] Contrary to the previous report,[15] the dimer model gave a much better fit and we obtained a dimer coupling (spin gap) $J_D = 61(2)$ K with the number of the dimers (N_D) = 0.25(1) per formula unit (f.u.), and the number of the spin segments that contribute the Curie–Weiss term (N_F) = 0.27(1) per f.u. These numbers describe well the spin configuration shown in Figure 6(d), in which almost 2 (0.2 f.u.) dimers and 2 (0.2 f.u.) spin segments are located statistically on the 10 Cu sites. To our knowledge, there is currently no theoretical approach for such a correlated, diluted spin system. However, the solid solution qualitatively shows a transition from an antiferromagnetically ordered state to a dimerlike state, as predicted by Haldane[22] for the $S = 1/2$ isotropic Heisenberg antiferromagnetic chain, with carrier doping. Neutron scattering experiments with single crystals are currently underway to rule out the spin dynamics of the solid solution.

In summary, we have succeeded in preparing the quasi-one-dimensional cuprates $(Ca_{1-x}Y_x)_{0.82}CuO_2$, with $0 \le x \le 0.435$, at room pressure. The structural parameters are slightly different from those recently reported for samples prepared under 215 bar of oxygen. However, the magnetic behavior is largely independent of the preparation conditions, but strongly dependent on the carrier concentration. Despite its crystal structure, the solid solution has a long-range correlation in the spin configuration. Upon carrier-doping, long-range magnetic ordering collapses and an isolated one-dimensional character appears. Further experimental and theoretical studies are now in progress to understand the properties of such a diluted spin system.

Experimental Section

Sample preparation: Samples were prepared from $CaCO_3$ (99.9%), Y_2O_3 (99.99%), and CuO (99.99%) powders. Intimate mixtures of these powders were heated at a temperature between 830 °C and 1000 °C for appropriate periods with intermediate grindings. All the samples were prepared in flowing oxygen at room pressure. Since the appearance of high-temperature stable phase Ca_2CuO_3 prevented the formation of Ca-rich solid solutions, the samples with $x \le 0.10$ were prepared at 830 °C for the total heating time of 360 h. The optimum sintering conditions were found to be closely dependent on the sample composition; the samples with $0.15 \le x \le 0.30$ and $0.30 < x \le 0.45$ were synthesized at 880 °C for 192 h and 980 °C for 144 h, respectively.

Characterization: X-ray powder diffraction (XRD) data were collected at room temperature in the angular range $10° - 100°$ with a 2θ step of 0.020° on a Siemens D5000 diffractometer. Rietveld analysis was carried out for the X-ray diffraction data with the Rietan-97 program.[17] Interatomic distances were computed with the program ORFFE.[23] The formal Cu valence of the samples was determined from the oxygen content of the samples measured by thermogravimetry under N_2-5% H_2 atmosphere. Magnetic susceptibility was measured with a SQUID magnetometer with field cool (FC) conditions under 1000 Oe of magnetic field from 300 K to 4 K.

Structure model: The basic structure was determined by the X-ray Rietveld analysis, excluding the peaks of superstructure. The structure model proposed by Babu and Greaves[11] is adopted. For example, the refined structural parameters of $Ca_{0.82}CuO_2$ are: space group *Fmmm* (No. 69); a = 2.80556(6) Å, b = 6.3208(1) Å, and c = 10.5765(2) Å; R_{WP} = 6.28%, R_P = 4.00%, R_e = 3.69% and R_I = 5.30%. Other relevant parameters are given in Table 1.

Table 1. Selected refined structural parameters for $Ca_{0.82}CuO_2$

Site	Atom	Occupancy	x	y	z	B
16*l*	Ca	0.205	0.390(1)	1/4	1/4	1.36(11)
4*a*	Cu	1.000	0	0	0	1.38(5)
16*m*	O	0.500	0	0.0480(7)	0.6222(3)	1.0

Acknowledgments

The authors thank Dr. A. J. Wright (School of Chemistry, University of Birmingham) for his help in the TGA measurement. This work was supported, in part, by the JSPS (Japan Society for the Promotion of Science) Post Doctoral Fellowships for Research Abroad and Merck.

[1] M. Uehara, T. Nagata, J. Akimitsu, H. Takahashi, N. Mori, K. Kinoshita, *J. Phys. Soc. Jpn*. **1996**, *65*, 2764–2767.
[2] For a recent perspective, see: S. Maekawa, *Science* **1996**, *273*, 1515.
[3] E. M. McCarron, III, M. A. Subramanian, J. C. Calabrese, R. L. Harlow, *Mat. Res. Bull*. **1988**, *23*, 1355–1365.
[4] N. E. Brese, M. O'Keeffe, R. B. von Dreele, V. G. Young, *J. Solid State Chem*. **1989**, *83*, 1–7.
[5] M. Kato, H. Chizawa, Y. Koike, T. Noji, Y. Saito, *Physica C* **1994**, *235–240*, 1327–1328.
[6] M. Kato, K. Shiota, Y. Koike, *Physica C* **1996**, *258*, 284–292.
[7] K. Kumagai, S. Tsuji, M. Kato, Y. Koike, *Phys. Rev. Lett*. **1997**, *78*, 1992–1995.
[8] Z. Hiroi, M. Azuma, M. Takano, Y. Bando, *J. Solid State Chem*. **1991**, *95*, 230–238.
[9] J. Karpinski, H. Schwer, G. I. Meijer, K. Conder, E. M. Kopnin, C. Rossel, *Physica C* **1997**, *274*, 99–106.
[10] T. Siegrist, R. S. Roth, C. J. Rawn, J. J. Ritter, *Chem. Mater*. **1990**, *2*, 192–194.
[11] T. G. N. Babu, C. Greaves, *Mat. Res. Bull*. **1991**, *26*, 499–506.
[12] J. G. Thompson, J. D. Fitz Gerald, R. L. Withers, P. J. Barlow, J. S. Anderson, *Mat. Res. Bull*. **1989**, *24*, 505–515.
[13] P. K. Davies, E. Caignol, T. King, *J. Am. Ceram. Soc*. **1991**, *74*, 569–573.
[14] P. K. Davies, *J. Solid State Chem*. **1991**, *95*, 365–387.
[15] J. Dolinsek, D. Arcon, P. Cevc, O. Milat, M. Miljak, I. Aviani, *Phys. Rev. B* **1998**, *57*, 7798–7803.
[16] A. Hayashi, B. Batlogg, R. J. Cava, *Phys. Rev. B* **1998**, *58*, 2678–2683.

0947-6539/99/0508-2268 $ 17.50+.50/0 *Chem. Eur. J.* **1999**, *5*, No. 8

[17] F. Izumi, in *The Rietveld Method*, (Ed: R. A. Young), Oxford University, Oxford **1993**, chapter 13.
[18] N. Motoyama, H. Eisaki, S. Uchida, *Phys. Rev. Lett*. **1996**, *76*, 3212–3215.
[19] F. C. Zhang, T. M. Rice, *Phys. Rev. B* **1988**, *37*, 3759- 3761.
[20] S. A. Carter, B. Batlogg, R. J. Cava, J. J. Krajewski, W. F. Peck, Jr., T. M. Rice, *Phys. Rev. Lett*. **1996**, *77*, 1378–1381.
[21] J. W. Hall, W. E. Marsh, R. R. Weller, W. E. Hatfield, *Inorg. Chem*. **1981**, *20*, 1033–1037.
[22] F. D. M. Haldane, *Phys. Rev. B* **1982**, *25*, 4925–4928.
[23] W. R. Busing, K. O. Martin, H. A. Levy, *Report ORNL-TM- 306*, Oak Ridge National Laboratory, TN, **1964**.

Received: September 17, 1998 [F1352]